24th COBEM - 2017

24th ABCM International Congress of Mechanical Engineering
December 3-8, 2017, Curitiba, PR, Brazil

COBEM-2017-1970
NUMERICAL SIMULATION OF MIXED CONVECTION IN CAVITY FILLED WITH HETEROGENEOUS AND HOMOGENEOUS POROUS MEDIUM

Renato Normandia Tavares
Fernando C. De Lai
Silvio L. M. Junqueira
Research Center for Rheology and Non-Newtonian Fluids (CERNN), Postgraduate Program in Mechanical and Materials Engineering (PPGEM), Federal University of Technology – Paraná (UTFPR), Curitiba, Brazil.
renato_normandia@hotmail.com, fernandodelai@utfpr.edu.br, silvio@utfpr.edu.br

Abstract. *In this work the mixed convection inside a sliding lid enclosure heated from below and filled with fluid-saturated porous medium according to the macroscopic and the microscopic approaches is numerically simulated. In the heterogeneous (microscopic) or continuum approach, the solid domain is represented by a set of heat conductive blocks equally spaced and surrounded by fluid. The porous-continuum (macroscopic) or homogeneous model is defined in a visual resolution that does not allow the identification of the solid-fluid interface, and thus can be considered as a single medium. Mass, momentum and energy balance equations are obtained in dimensionless form to represent both the continuum and the porous-continuum models. The numerical solution is obtained via finite volume method. The QUICK interpolation scheme is set for numerical treatment of the advection terms and the SIMPLE algorithm is applied for pressure-velocity coupling. Considering the Prandtl number and laminar regime, the effects of varying Reynolds ($10^2 \leq Re \leq 10^3$) and Rayleigh ($10^3 \leq Ra \leq 10^6$) numbers for both approaches are presented. The permeability is obtained using the number of blocks ($9 \leq N \leq 64$) and the Darcy number for a fixed fluid volumetric fraction. Expressions for the average Nusselt number for both the continuum and the porous-continuum models as a function of Ra_K for each Re are obtained.*

Keywords: *mixed convection, porous medium, heterogeneous, homogeneous, numerical simulation.*

1. INTRODUCTION

Studies on the mixed convection process in fluid-saturated porous media have been an important issue over the past decades. As pointed out by Lai (2000), a variety of researches ranging from geothermal reservoirs and nuclear waste repository (Lai and Kulacki, 1991) to solar power collectors and the cooling electronics (Mahmud and Pop, 2006), to name a few, arose due to the need to better interpret the interactions between buoyancy and inertia inside a porous substrate. For the present work, two approaches to model the porous substrate are considered. The heterogeneous model, referred in the literature as a continuum or microscopic model consists of two distinct phases (solid and fluid), idealizing a domain formed by a connected network of pores in a disconnected solid matrix, represented by heat conductive square obstacles (Merrikh and Lage, 2005; Junqueira *et al*., 2013; Poletto *et al*., 2015; Lage *et al*., 2016).

The porous-continuum model, also known in the literature as homogeneous or macroscopic, considers the solid and the fluid phases as a single medium, approaching the problem in a scale where the geometric nuances, such as the interface between the two phases are disregarded (Nithiarasu *et al*., 1997; Chen *et al*., 2009; Dias *et al*., 2010; De Lai *et al*., 2011; Lima *et al*., 2014).

In the present work the mixed convection in a top sliding lid enclosure, heated from below and filled with fluid-saturated porous medium is investigated. The thermal process according to the homogeneous and heterogeneous approaches is compared in terms of the heated surface average Nusselt number.

Aiming the laminar regime and a unitary Prandtl number, the flow parameters are kept in the range of Reynolds ($10^2 \leq Re \leq 10^3$) and Rayleigh ($10^3 \leq Ra \leq 10^6$) numbers for both approaches. For the continuum one, values of permeability are obtained by varying the number of blocks N from 9 to 64 for a fixed fluid volumetric fraction (φ=0.64); in the porous-continuum substrate the Darcy number (Da) is estimated in terms of N and φ. Numerical results of the comparative study between the two approaches allow obtaining average Nusselt number expressions for both the continuum and the porous-continuum models as a function of $Ra_K = Ra \times Da$ for each Re.

2. PROBLEM FORMULATION

Figure 1 displays both the heterogeneous (a) with N=16 solid blocks and homogeneous (b) domains. The square cavity (H/L=1), is heated from below (θ=1) with adiabatic vertical surfaces $(\partial\theta/\partial X = 0)$; the top lid moves with constant speed (U=1).

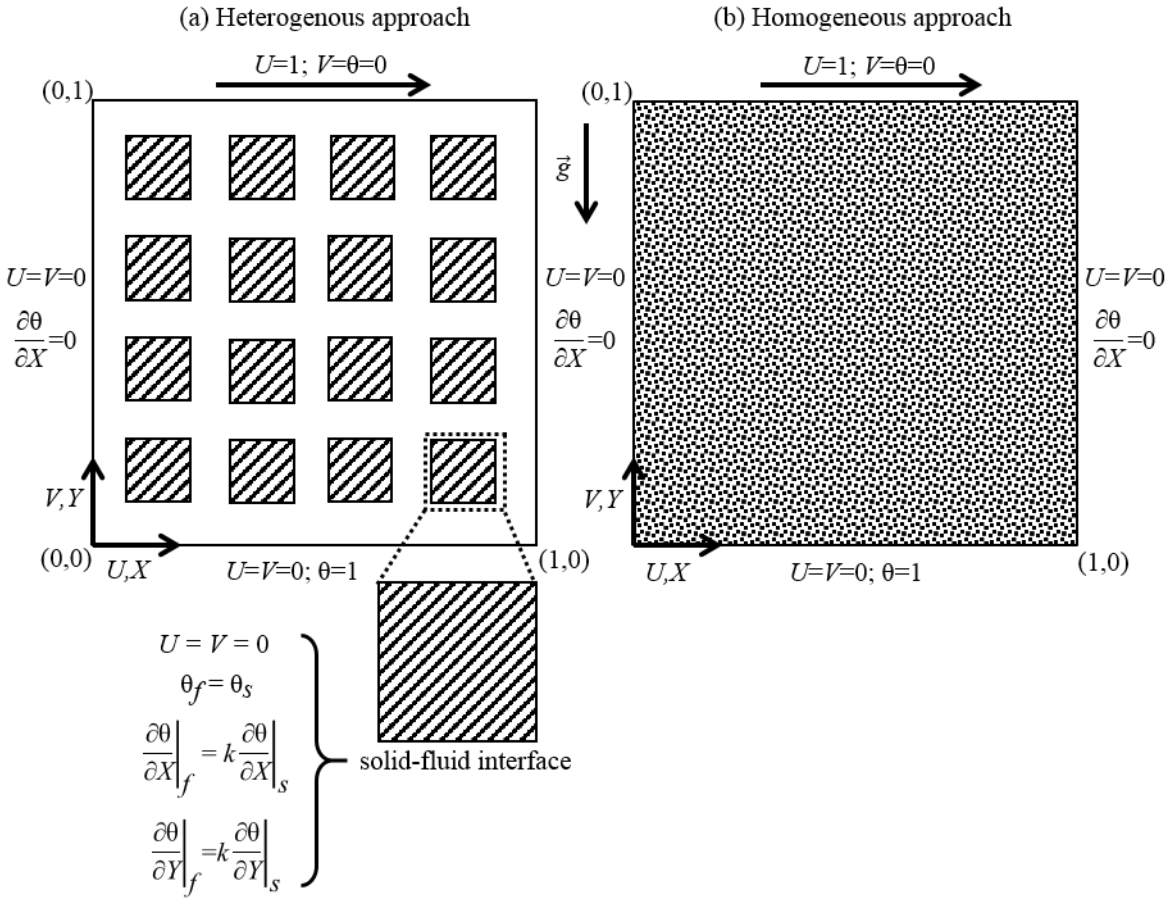

Figure 1. Problem geometry and boundary conditions: (a) Continuum and (b) Porous-continuum approach.

Variables U, V, θ, g and k are the horizontal and vertical dimensionless wall velocities, dimensionless temperature, gravity acceleration and solid-fluid thermal conductivity ratio, respectively.

The problem is Cartesian two-dimensional and the flow is monophasic, laminar and steady for a Newtonian and incompressible fluid with constant properties. The Oberbeck-Boussinesq approximation models the density variation (Bejan, 2013); the gravity acts in the vertical direction and the viscous dissipation term is neglected and the solid blocks are considered isotropic and heat conductive.

In the heterogeneous approach, the cavity is filled with heat conductive, impermeable, rigid and equally spaced square blocks. According to such model, the dimensionless balance equations are applied separately for the fluid (Eq. 1-4) and solid (Eq. 5) constituents.

$$\frac{\partial U}{\partial X}+\frac{\partial V}{\partial Y}=0 \tag{1}$$

$$U\frac{\partial U}{\partial X}+V\frac{\partial U}{\partial Y}=-\frac{\partial P}{\partial X}+\frac{1}{Re}\left(\frac{\partial^2 U}{\partial X^2}+\frac{\partial^2 U}{\partial Y}\right) \tag{2}$$

$$U\frac{\partial V}{\partial X}+V\frac{\partial V}{\partial Y}=-\frac{\partial P}{\partial Y}+\frac{1}{Re}\left(\frac{\partial^2 V}{\partial X^2}+\frac{\partial^2 V}{\partial Y}\right)+\frac{Ra}{PrRe^2}\theta \tag{3}$$

$$U\frac{\partial\theta}{\partial X}+V\frac{\partial\theta}{\partial Y}=\frac{1}{RePr}\left(\frac{\partial^2\theta}{\partial X^2}+\frac{\partial^2\theta}{\partial Y}\right) \tag{4}$$

$$\frac{\partial^2\theta}{\partial X}+\frac{\partial\theta^2}{\partial Y}=0 \tag{5}$$

The following dimensionless variables can be written:

$$(X,Y)=\frac{(x,y)}{L};\ (U_f,V_f)=\frac{(u_f,v_f)}{U_o};\ P_f=\frac{p_f}{\rho_f U_o^2};\ \theta=\frac{(\langle T\rangle-T_F)}{(T_Q-T_F)} \tag{6}$$

where L, U_o, $\rho_f U_o^2$ and T_f are characteristic cavity length, lid driven surface velocity, dynamic pressure and reference temperature, respectively. In the Equations (2)-(4) the following non-dimensional groups, respectively, Prandtl, Reynolds and Rayleigh numbers are identified:

$$Pr=\frac{\nu_f}{\alpha};\ Re=\frac{U_o L}{\nu_f};\ Ra=\frac{Pr(T_Q-T_F)\beta g L^3}{\nu_f{}^2} \tag{7}$$

Considering thermal equilibrium between the solid and fluid phases, the non-dimensional form of the balance equations for the macroscopic approach, obtained using the volumetric average theory (Whitaker, 1986), can be written as follow:

$$\frac{\partial\langle U_f\rangle}{\partial X}+\frac{\partial\langle V_f\rangle}{\partial Y}=0 \tag{8}$$

$$\frac{1}{\varphi^2}\left(\langle U_f\rangle\frac{\partial\langle U_f\rangle}{\partial X}+\langle V_f\rangle\frac{\partial\langle U_f\rangle}{\partial Y}\right)=-\frac{\partial\langle P_f\rangle^f}{\partial X}+\frac{1}{\varphi Re}\left(\frac{\partial^2\langle U_f\rangle}{\partial X^2}+\frac{\partial^2\langle U_f\rangle}{\partial Y^2}\right)-\frac{\langle U_f\rangle}{ReDa}-\frac{C_F}{\sqrt{Da}}\left|\langle U_f\rangle\right|\langle U_f\rangle \tag{9}$$

$$\frac{1}{\varphi^2}\left(\langle U_f\rangle\frac{\partial\langle V_f\rangle}{\partial X}+\langle V_f\rangle\frac{\partial\langle V_f\rangle}{\partial Y}\right)=-\frac{\partial\langle P_f\rangle^f}{\partial Y}+\frac{1}{\varphi Re}\left(\frac{\partial^2\langle V_f\rangle}{\partial X^2}+\frac{\partial^2\langle V_f\rangle}{\partial Y^2}\right)-\frac{\langle V_f\rangle}{ReDa}-\frac{C_F}{\sqrt{Da}}\left|\langle V_f\rangle\right|\langle V_f\rangle+\frac{Ra}{PrRe^2}\theta \tag{10}$$

$$\langle U_f\rangle\frac{\partial\theta}{\partial X}+\langle V_f\rangle\frac{\partial\theta}{\partial Y}=\frac{1}{RePr}\left(\frac{\partial^2\theta}{\partial X^2}+\frac{\partial^2\theta}{\partial Y^2}\right) \tag{11}$$

where Da, C_F and K are the Darcy number, Forchheimer coefficient and the effective permeability, respectively (Eq. 12). Also, $\langle U_f\rangle$, $\langle V_f\rangle$ are, respectively, the averaged velocity at X and Y direction. $\langle P_f\rangle$ represents the pressure and θ the temperature, both considered as average values.

$$Da=\frac{K}{L^2};\ C_F=\frac{1.75}{(150\varphi^3)^{1/2}};\ K=\frac{[1-(1-\varphi)^{0.5}]^3 D^2}{12(1-\varphi)} \tag{12}$$

The heat transfer through the cavity can be measured by the average Nusselt number at the heated wall:

$$\overline{Nu}=-\int_0^1\left.\frac{\partial\theta}{\partial Y}\right|_{Y=0}dX \tag{13}$$

The flow dynamic behavior is studied through streamlines, define as:

$$\Psi=\int_0^1 U dY=-\int_0^1 V dX \tag{14}$$

Numerical solutions for the equations (1)-(5) and (8)-(11) are obtained via the finite volume method. The QUICK scheme is employed to deal with the convective terms and the SIMPLE algorithm is applied to the pressure and velocity

coupling. The convergence criteria adopted was $R^{\Theta}<10^{-3}$ for mass conservation and momentum and $R^{\Theta}<10^{-6}$ for energy conservation, being R^{Θ} defined as:

$$R^{\Theta} = \frac{\sum_P \left| \sum_{nb} a_{nb}\Theta_{nb} + S_c - a_p\Theta_p \right|}{\sum_P \left| a_p\Theta_P \right|} \tag{15}$$

where R^{Θ}, a_{nb}, Θ and S_c are, respectively, the residuals, coefficients, variables and source term defined as $S_c=S_p\,\Theta - S_{\Theta}$.

3. RESULTS AND DISCUSSION

The validation of both the methodology and the numerical code were achieved comparing results with two classic configurations found in literature, as observed in Tables 1, 2 and 3. Results for an enclosure filled with heat conductive square solid blocks immersed in fluid (Table 1), a cavity with homogeneous porous medium (Table 2) and for a top sliding lid square cavity heated from below (Table 3) are presented. The closeness between the results gives credibility to the numerical procedure not only in dealing with the convection process in both continuum and porous-continuum domains but also to represent the mixed convection process.

Table 1. Verification results: $\overline{Nu}$ for heterogeneous cavity (φ=0.64 and Pr=1).

N	Ra	Merrikh and Lage (2005)	Junqueira et al. (2013)	Present
9	10^5	1.383	1.397	1.396
	10^6	6.164	6.255	6.271
	10^7	16.087	16.019	16.082
	10^8	31.797	30.914	31.373
16	10^5	1.233	1.244	1.244
	10^6	4.274	4.347	4.371
	10^7	15.258	15.208	15.285
	10^8	31.180	30.488	30.972
36	10^5	1.098	1.107	1.107
	10^6	2.626	2.643	2.666
	10^7	11.798	11.895	12.071
	10^8	30.689	29.952	30.530
64	10^5	1.051	1.048	1.048
	10^6	2.223	2.192	2.219
	10^7	8.094	7.947	8.034
	10^8	29.394	28.671	29.236

Table 2. Verification results: $\overline{Nu}$ for homogeneous cavity heated on the side (Pr=1).

φ	Da	Ra	Nithiarasu *et al.* (1997)	Chen *et al.* (2009)	Present
0.4	10^{-2}	10^3	1.010	1.010	1.008
		10^5	2.983	2.990	2.994
	10^{-4}	10^5	1.067	1.064	1.064
		10^7	7.810	7.860	7.771
	10^{-6}	10^7	1.079	1.078	1.078
0.6	10^{-2}	10^3	1.015	1.012	1.012
	10^{-4}	10^5	1.071	1.070	1.067
		10^6	2.725	2.714	2.705
	10^{-6}	10^7	1.079	1.078	1.078
0.9	10^{-2}	10^3	1.023	1.020	1.018
		10^4	1.640	1.630	1.632
		10^5	3.910	3.920	3.918
	10^{-4}	10^5	1.072	1.071	1.069
		10^7	9.202	9.490	9.318
	10^{-6}	10^7	1.080	1.080	1.078

Table 3. Verification results: $\overline{Nu}$ for cavity with sliding lid heated from below (Pr=1).

Re	*Gr*	Iwatsu *et al.* (1993)	Poletto *et al.* (2016)	Present
100	10^2	1.940	2.039	2.039
	10^4	1.340	1.400	1.400
	10^6	1.020	1.020	1.020
400	10^2	3.840	4.082	4.081
	10^4	3.620	3.843	3.843
	10^6	1.220	1.181	1.181
1000	10^2	6.330	6.579	6.578
	10^4	6.290	6.530	6.529
	10^6	1.770	1.762	1.762

Concerning the mixed convection in clear cavity heated from the bottom, numerical results obtained by Cheng (2011) indicated that the increasing of average Nusselt is not continuous, since a sudden fall in the average Nusselt accompanied by a separation in the flow occurs. Such phenomenon, denominated Hopf bifurcation, usually begins in a small circulation region in the right bottom corner and quickly disperses throughout the cavity.

In Figure 2, using uniform mesh of 256x256 control volumes, one can verify the values of *Re* and *Gr* that correspond to the flow separation (the average Nusselt drops), considering the Richardson number $Ri = (Gr \cdot Re^{-2}) = 1$ and $Pr = 0.71$.

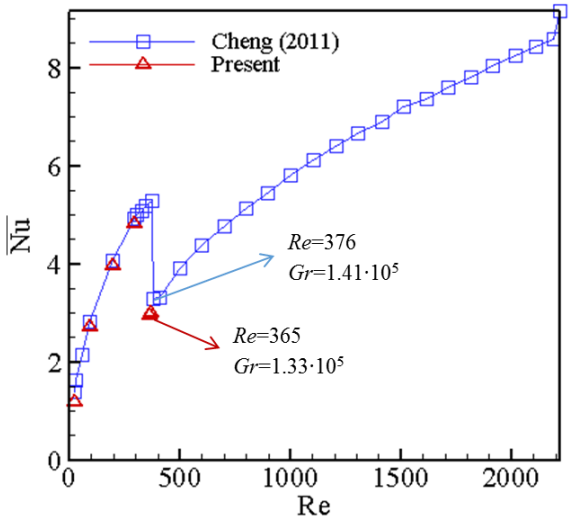

Figure 2. Average Nusselt number ($\overline{Nu}$) in function of *Re* and *Gr*: Hopf bifurcation for $Ri = 1$.

In general, for the homogeneous cavity, the reduction of the average Nusselt number happens mainly due to the Hopf bifurcation. In Figure 3 a primary vortex occurs as the top wall displaces and a secondary one is originated with the separation of the flow near the right inferior corner (for *Re*=500 and 1000). Such separation of the flow and the consequent decrease of the average Nusselt are linked to the natural and forced convection effects, whose combination not necessarily results in the increase of heat transfer in the cavity.

In configurations presenting the flow separation, the accumulation of isotherms on the bottom right and on top left regions denotes the presence of the forced convection thermal boundary layer.

Figure 4 (*Re*=1000 and $Ra=10^6$) displays the streamlines and isotherms for the heterogeneous cavity considering 9, 16, 36 and 64 obstacles and also for the homogeneous cavity for different values of *Da*. Remarkably, in both approaches the flow separation is observed at the right of the bottom region, characterizing the occurrence of the Hopf bifurcation as the permeability increases.

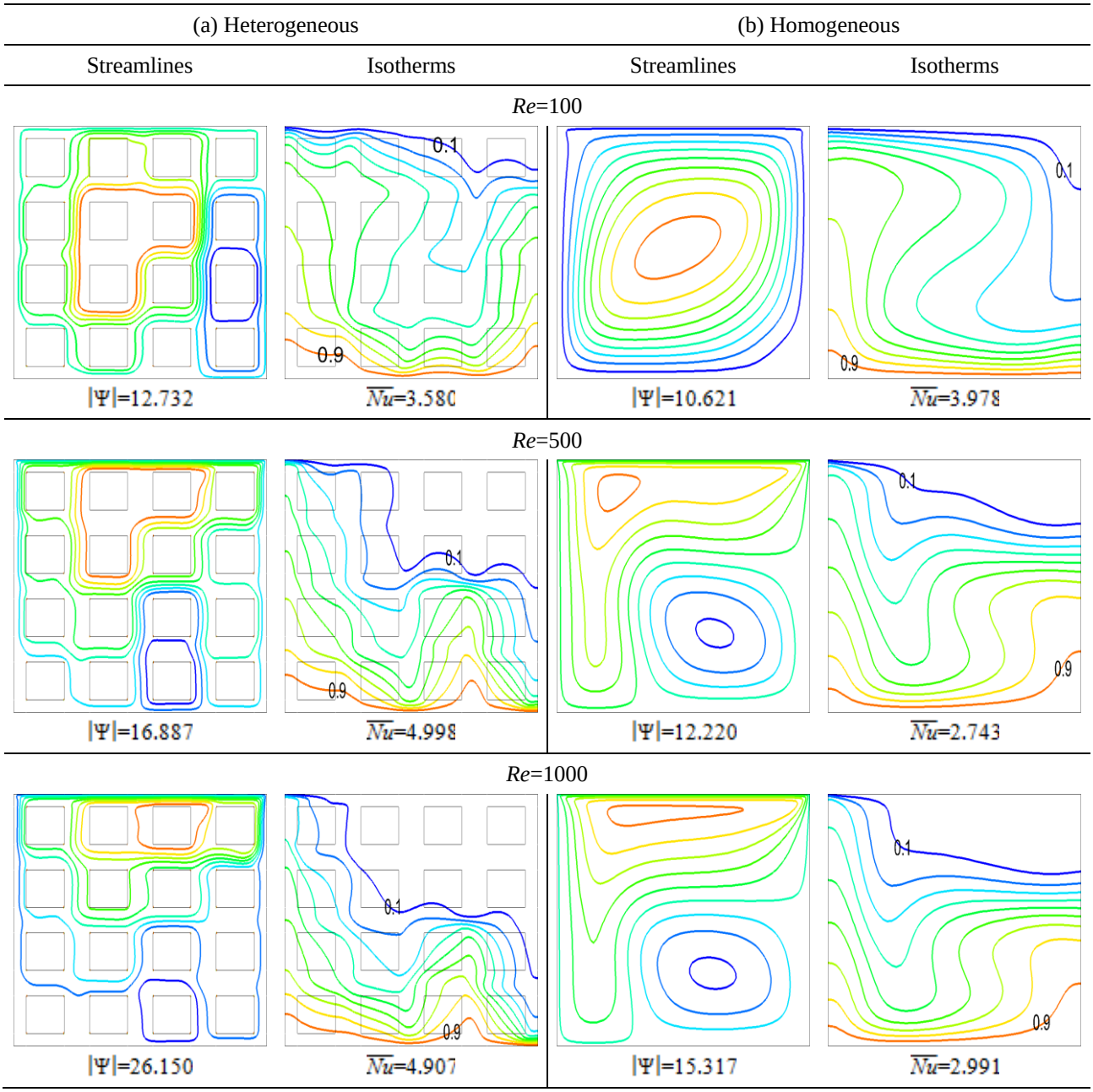

Figure 3. Reynolds number effect over streamlines and isotherms for: (a) heterogeneous and (b) homogeneous cavities, considering $Ra=10^6$, $\varphi=0.64$, $N=16$ and $Da=3.33\text{x}10^{-4}$.

Considering the macroscopic (homogeneous) medium the secondary flow increases directly as the permeability increases, whilst for the heterogeneous medium the primary flow tends to fill the cavity, limiting the growth of the secondary flow. The permeability increasing also implies in the divergence between the values of average Nusselt observed in the heterogeneous and the homogeneous approaches. Indeed, in this case the fluid flows easily through blocks regions, where streamlines are concentrated. The isotherms approximation denotes that the heat transfer increases and the flow separation results in distorted isotherms distribution, mainly on the interface regions between the primary and the secondary flows.

The influence of the sliding-lid displacement can also be visualized in Figure 4 ($N=64$ and $Da=8.333\text{x}10^{-5}$), as the first isotherm is placed away from the top region, denoting a small temperature gradient due to the high fluid circulation. As a matter of fact, in this region the streamlines are displaced in the same direction as the top wall.

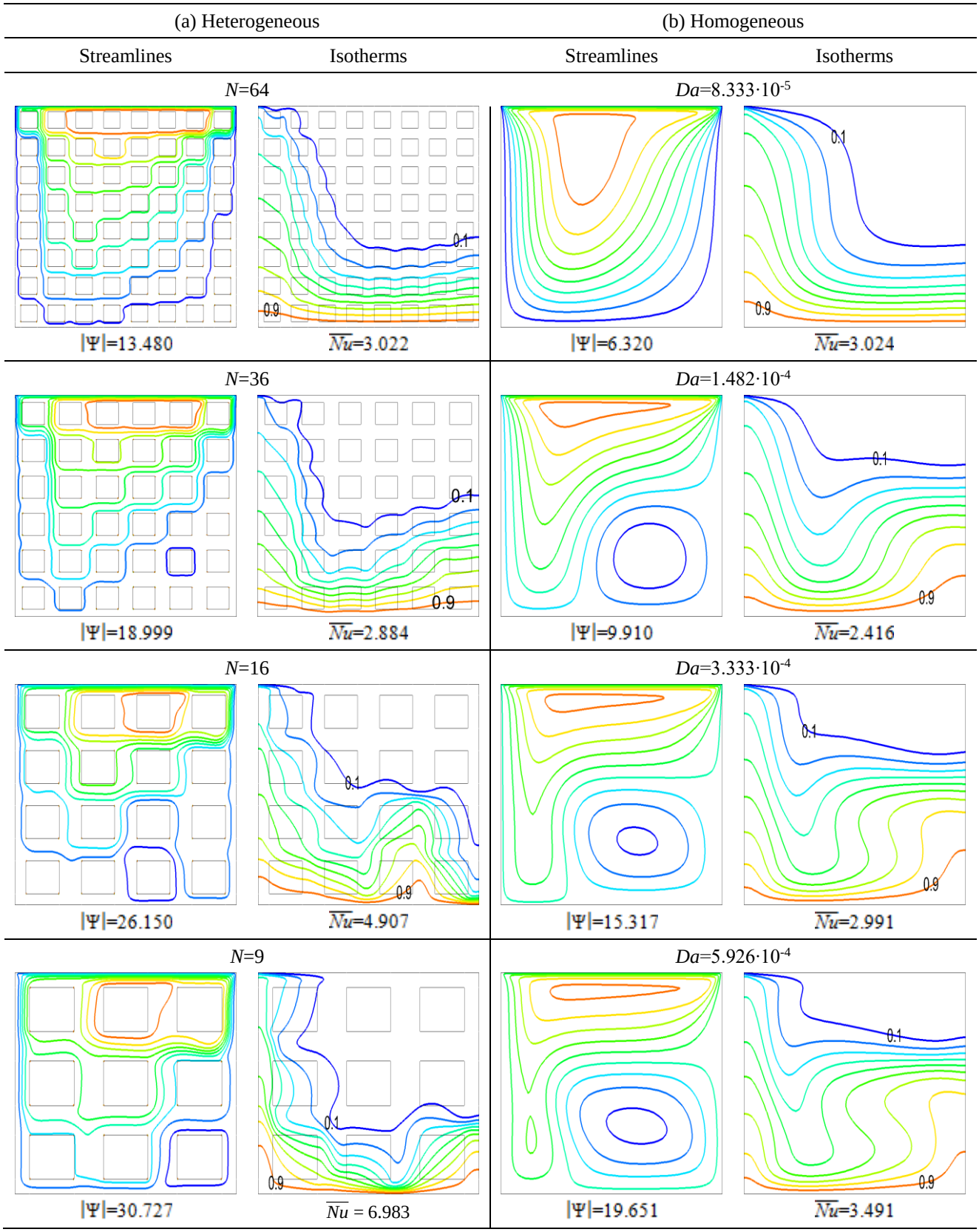

Figure 4. Permeability effect over streamlines and isotherms for: (a) heterogeneous and (b) homogeneous cavities, considering Re=1000, Ra=10^6 and φ=0.64.

A non-linear regression of the average Nusselt ($\overline{Nu}$) is applied to obtain continuous functions in terms of Rayleigh and Darcy numbers for a certain Reynolds number. Figure 5 displays curves of the analytical expressions of $\overline{Nu}$ for both the heterogeneous and the homogeneous approaches, as a function of Ra_K=Ra×Da, for Re=100, 500 and 1000.

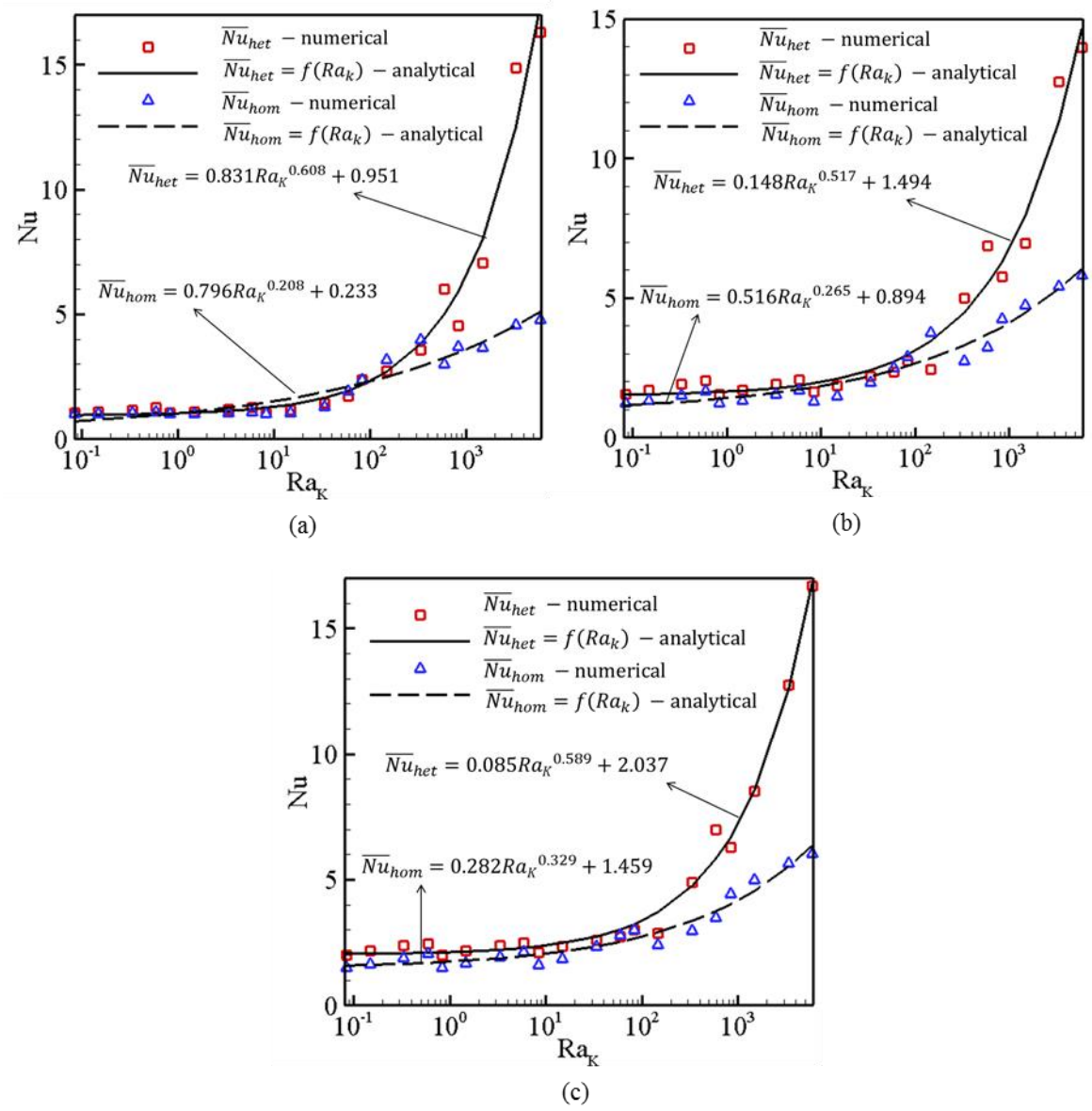

Figure 5. Analytical expression of $\overline{Nu}$ for heterogeneous and homogeneous cavities:
(a) Re=100, (b) Re=500 and (c) Re=1000.

4. CONCLUSIONS

In this work the problem of mixed convection in heterogeneous and homogeneous cavities was investigated. For that, numerical simulations were done in a top-sliding lid cavity heated from the bottom. The heterogeneous enclosure is filled with solid, rigid, impermeable, heat conductive and equally spaced square obstacles. The homogeneous cavity is modeled according to a porous-continuous approach. Finally, analytical expressions for the average Nusselt number were obtained in function of the Darcy-Rayleigh number for each Reynolds number.

From results have shown that the $\overline{Nu}$ drops abruptly with the flow separation (Hopf bifurcation), an indication that the appearance of the two flow recirculation regions acts as a thermal isolation between the heated (bottom) surface and the cooled (top) one. In addition, the rise of the Hopf bifurcation is not enough to provoke the abrupt decrease of the average Nusselt, however is sufficient to limit the increase of the heat transfer.

The comparison between the two approaches showed that, in most of the cases, the heterogeneous cavity exchanges more heat than the homogeneous one, mainly for higher values of Reynolds, Rayleigh and Darcy. Indeed, for higher

permeability values or less quantity of solid obstacles, the discrepancy between the two approaches is more evident as the gap between blocks, in the heterogeneous cavity, channelizes the flow between them.

Finally, the choice of the best approach to represent the porous medium must be done carefully, since the lack of information of the homogeneous approach is an important matter. On the other hand, the low computational cost required by the homogeneous approach is quite attractive, especially when the solid-fluid geometry interface is complex or the substrate sample is not accessible.

5. ACKNOWLEDGEMENTS

The authors would like to acknowledge the support of IRF/CENPES/PETROBRAS, the PRH-ANP/MCT program (PRH10-UTFPR) and the National Council for Scientific and Technological Development (CNPq).

6. REFERENCES

Bejan, A. Convection Heat Transfer. 4th ed., Wiley, 2013.

Chen, X.B., Yu, P., Sui, Y., Winoto, S.H. Low. Natural convection in a cavity filled with porous layers on the top and bottom walls. Transport Porous Med. 78(2), (2009) 259-276.

Cheng, T. S. Characteristics of mixed convection heat transfer in a lid-driven square cavity with various Richardson and Prandtl numbers. Int. J. Therm. Sci. 50 (2011) 197-205.

De Lai, F. C., Junqueira, S. L. M., Franco, A. T., Lage, J. L., Waldmann, A. T. A. and Martins, A. L. Convecção natural em cavidade porosa fraturada utilizando modelos micro e macroscópico. In: XXXV Congresso Brasileiro de Sistemas Particulados - ENEMP, 2011, Vassouras, RJ. Anais do ENEMP, 2011.

Dias, R., De Lai, F.C., Junqueira, S.L.M., Franco, A.T., Martins, A.L., Lomba, R.F.T. and Lage, J.L. Natural convection in a cavity filled with a bi-dispersed porous medium. Proceedings of the Rio Oil & Gas Expo and Conference, Rio de Janeiro, RJ (2010).

Iwatsu, R., Hyun, J.M. and Kuwahara, K. Mixed convection in a driven cavity with a stable vertical temperature gradient. Int. J. Heat Mass Transf. 36 (1993) 1601-1608.

Junqueira, S.L.M., De Lai, F.C., Franco, A.T. and Lage, J.L. Numerical investigation of natural convection in heterogeneous rectangular enclosures. Heat Transfer Engineering, 34(5-6), (2013) 460-469.

Lage, J.L., Junqueira, S.L.M., De Lai, F.C. and Franco, A.T. Aspect ratio effect on the prediction of boundary layer interference in steady natural convection inside heterogeneous enclosures. Int. J. Heat Mass Transf. 92 (2016) 940–947.

Lai, F.C. Mixed convection in saturated porous media. In: K.Vafai, Ed. Handbookof Porous Media, 1st edn. New York: Marcel Dekker. (2000) 605-662.

Lai, F.C., Kulacki, F.A. Experimental study of free and mixed convection in horizontal porous layers locally heated from below. Int. J. Heat Mass Transfer. 34(2), (1991) 525-541.

Lee, J.R. and Ha, M.Y. A numerical study of natural convection in a horizontal enclosure with a conducting body. Int. J. Heat Mass Transf. 48 (2005) 3308-3318.

Lima, G. H., De Lai, F. C., Franco, A. T. and Junqueira, S. L. M. Convecção natural em substrato poroso fraturado com aquecimento por baixo. In: Rio Oil & Gas Expo and Conference, 2014, Rio de Janeiro, RJ. Proceedings of Rio Oil & Gas, 2014.

Mahmud, S. and Pop, I. Mixed convection in a square vented enclosure filled with a porous medium. Int. J. Heat Mass Transfer. 49 (2006) 2190-2206.

Merrikh, A.A. and Lage, J.L. Natural convection in an enclosure with disconnected and conducting solid blocks. Int. J. Heat Mass Transf. 48 (2005) 1361-1372.

Nithiarasu, P., Seetharamu, K.N. and Sundararajan, T. Natural convective heat transfer in a fluid saturated variable porosity medium. Int. J. Heat Mass Transf. (1997) 3955-3967.

Poletto, V.G., De Lai, F.C., Franco A.T., Junqueira and S.L.M. Numerical simulation of the convection in a non-homogeneous lid-driven square cavity subjected to a gravitational stable condition, in ASME 2016 HTSC, FE & ICNMM, Washington, D.C., 1, (2016) V001T03A007.

Poletto, V.G., De Lai, F.C., Franco A.T., Junqueira and S.L.M. Convection analysis in a lid-driven cavity partially filled with a conductive and centered solid block. In: 23rd ABCM International Congress of Mechanical Engineering, 2015, Rio de Janeiro.

Whitaker, S. Flow in Porous Media 1: A Theorical Derivation of Darcy's Law. Transport in Porous Media, p. 3-25, 1986.

7. RESPONSIBILITY NOTICE

The authors are the only responsible for the printed material included in this paper.